Control and Cybernetics
vol. **30** (2001) No. 2

Non-linear model of the N_2-laser excitation circuit

by

T. Niewierowicz, L. Kawecki and J. de la Rosa

Postgraduate Studies Section, Instituto Politécnico Nacional
07738 México, D.F., Mexico

Abstract: This paper presents a non-linear model of the Blumlein circuit for the excitation of an N_2-laser that leads to a high order integer-differential equation system where each of the two discharges (the spark gap and the laser chamber) taking place in the circuit are simulated by an inductance and a resistance connected in series. The inductance and the resistance of each loop are considered current dependent and their time behaviour is found by means of a parametric identification method based on the voltages measured in the charge capacitors. A comparison between two representations of the induced *emf* in the different loops of the circuit is used. The first one is based on the dynamical (or derivative) inductivity and the second one on the statical (or integrative) inductivity. A Gauss–Seidel algorithm for the parametric identification was used.
Keywords: non-linear models, lasers, parametric identification.

1. Introduction

For the pulsed excitation of N_2, a well-known arrangement is the Blumlein circuit. Its role is to produce a very intense uniform glow discharge across the laser head during a very short time. The Blumlein circuit consists of two common non-linear elements, a spark gap whose function is to fire the circuit and the laser chamber where the laser discharge takes place. Besides, in order to charge the circuit, a coil L parallel to the laser head is used. So, the circuit is reduced to two loops, which follow the fourth order differential equations for any voltage and current in the circuit, when each discharge taking place in the circuit is simulated by an inductance and a resistance connected in series, whose values are considered time independent.

Recently, Persephonis et al. (1995), have proposed to solve the integer-differential equations of a charge transfer circuit for the excitation of a N_2 laser by considering the behaviour of the inductances and resistances of the spark gap and the laser chamber as time dependent. They substituted the derivatives of the experimental circuit voltages in the equations at four very closed adjacent time instants, considering that during this short time interval the resistances

and inductances vary linearly, and solved the four equations for the unknown inductances and resistances at the corresponding time interval. By repeating the same procedure for other time intervals and scanning the entire time region of the discharge, the time histories of the resistances and inductances of the discharge were obtained.

In conventional electric circuits inductances are usually constant. In plasma systems this is generally not the case and for rapidly moving plasmas dL/dt can be very large (see Glasstone and Louberg, 1960; de la Rosa et al., 1994), so we consider the induced *emf* in the loops of the circuit as given by the Lenz law, where two different representations of the non-linear inductivity can be worked out.

In this work we propose the analysis of the complete Blumlein circuit considering the resistances and the inductances used to simulate the spark gap and laser chamber as time dependent. In fact, we use a p-order dependence of their values on the current. The resulting integer-differential equations of the system are solved through a parametric identification method based on the measured voltages in the capacitors C_1 and C_2. A Runge–Kutta method for solving the integral terms and a Gauss–Seidel algorithm (see Niewierowicz et al., 1995) were used for parametric identification.

2. Theoretical considerations

Figs. 1 and 2 show the experimental arrangement and the equivalent circuit of a N_2 laser excited by a Blumlein circuit. The circuit is composed of a spark gap (S. G.), the laser head, two capacitors and a coil L. When high voltage is applied, both capacitors are equally charged until the breakdown voltage across S. G. is reached. At this potential, the S. G. fires and C_2 begin to discharge very fast through S. G., so does C_1, but through L and S. G. in a slower way. A very quickly rising high voltage difference appears across the laser head until the laser breakdown voltage is reached and the discharge takes place. Fig. 3 shows the voltages V_{C1} and V_{C2} in the capacitors C_1 and C_2.

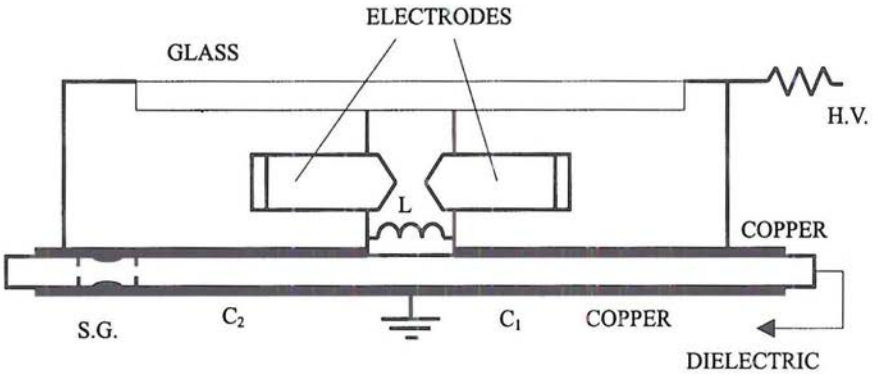

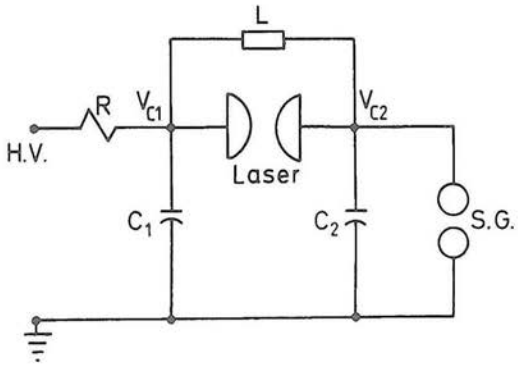

Figure 2. Equivalent circuit of an N_2 laser

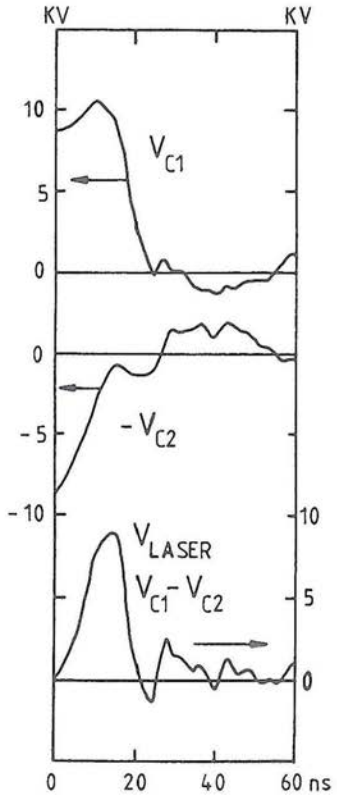

Figure 3. From top to bottom:
— voltage appearing at C_1 (V_{C1})
— voltage appearing at C_2 (V_{C2})

The voltages V_{C1} and V_{C2} were measured with two equal high voltages probes (Tektronix P6015) combined with a 300 MHz bandwidth oscilloscope (Tektronix 2440). The voltage in the laser head (see Fig. 3) is the voltage difference $V_{C1} - V_{C2}$ that was automatically given by the oscilloscope and is the average of 16 discharges. Stable operation of the laser was achieved at voltages ranging from 6 to 12 kV, pressures between 60 and 130 hPa and frequencies up to 20 Hz. The pulse-to-pulse fluctuations of the laser head voltage were smaller than 5%.

To analyse the circuit, each discharge taking place in the circuit is simulated by a non-linear inductance and resistance connected in series (see Fig. 4). R_1 and L_1 stand for the inductance and a resistance associated with the laser head loop, respectively, and R_2 and L_2 stand for the analogous parameters of the spark gap loop.

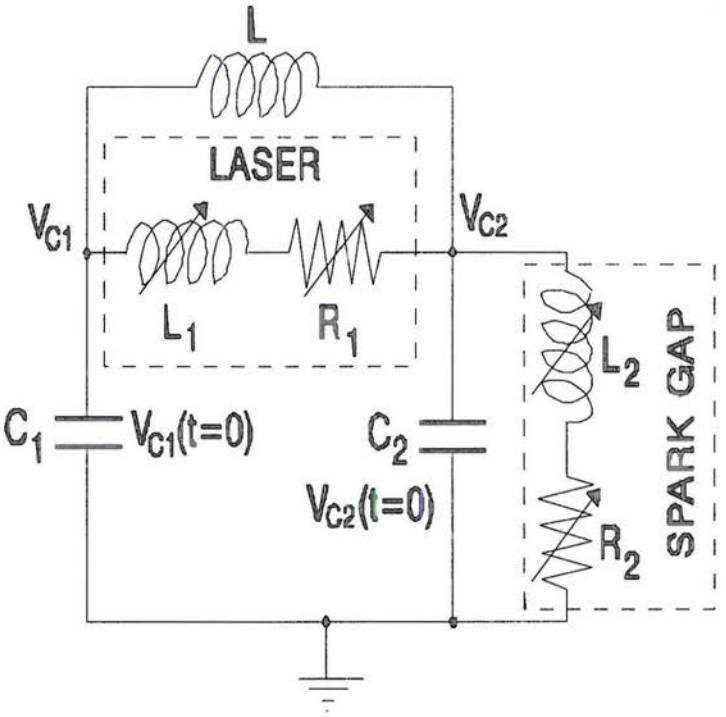

Figure 4. Equivalent circuit of the Blumlein circuit

The changes of R_1 and R_2 in both discharges are due to the change in the electron and ion concentrations, which produce a time and space dependence of

we take R_1 and R_2 as current dependent, and a form of power series for R_1 and R_2 is proposed.

$$\begin{aligned} R_1 &= f_{R_1}(I_1) \\ &= R_{1,p}I_1^p + R_{1,p-1}I_1^{p-1} + R_{1,p-2}I_1^{p-2} + \ldots + R_{1,1}I_1 + R_{1,0} \end{aligned} \tag{1}$$

$$\begin{aligned} R_2 &= f_{R_2}(I_2) \\ &= R_{2,p}I_2^p + R_{2,p-1}I_2^{p-1} + R_{2,p-2}I_2^{p-2} + \ldots + R_{2,1}I_2 + R_{2,0} \end{aligned} \tag{2}$$

Non-linear inductances can therefore be given through (see Wojnar, 1969):

$$\begin{aligned} U &= \frac{d\psi}{dt} = \frac{d[L_{int}(I)I]}{dt} = I\frac{dL_{int}(I)}{dt} + L_{int}(I)\frac{dI}{dt} && \text{3a)} \\ U &= \frac{d\psi}{dI}\frac{dI}{dt} = L_{der}(I)\frac{dI}{dt} && \text{3b)} \end{aligned} \tag{3}$$

where: L_{int}—is the integral inductance, L_{der}—is the derivative inductance, ψ—is the induced magnetic flux in the loop.

Eq. (3a) is the Faraday law of electromagnetic induction. This is independent of the way in which the flux is changed, the circuit may be distorted or moved, or the value of B (the magnetic induction) at various points inside the circuit may be changed. Equation (3b) is valid for a rigid stationary circuit, where the changes in flux result from changes in the current (see Reitz and Milford, 1960). In order to find which of the two representations produces the best fitting to the experimental laser voltage, we solve our model for both of them. The inductances L_1 and L_2 are represented through a power series too. Such expansion gives:

$$\begin{aligned} L_1 &= f_{L_1}(I_1) \\ &= L_{1,p}I_1^p + L_{1,p-1}I_1^{p-1} + L_{1,p-2}I_1^{p-2} + \ldots + L_{1,1}I_1 + L_{1,0} \end{aligned} \tag{4}$$

$$\begin{aligned} L_2 &= f_{L_2}(I_2) \\ &= L_{2,p}I_2^p + L_{2,p-1}I_2^{p-1} + L_{2,p-2}I_2^{p-2} + \ldots + L_{2,1}I_2 + L_{2,0} \end{aligned} \tag{5}$$

The differential equations governing the performance of the circuit are given as follows:

The first step ($0 \leq t \leq t_B$):

At $t = 0$ the S. G. fires and at $t = t_B$ the laser head fires. For this step, the equivalent circuit showing the operation of the system is shown in Fig. 5a. The equations governing its performance are given as follows (considering 3a):

$$R_2 I_2 + \beta I_2 \frac{dL_2}{dt} + L_2\frac{dI_2}{dt} + \frac{1}{C_2}\int_0^{t_B}(I_2 - I_{11})\,dt + V_2|_{t=0} = 0 \tag{6}$$

$$L\frac{dI_{11}}{dt} + \frac{1}{\quad}\int^{t_B} I_{11}\,dt + \frac{1}{\quad}\int^{t_B}(I_{11} - I_2)\,dt + V_1|_{t=0} + V_2|_{t=0} \tag{7}$$

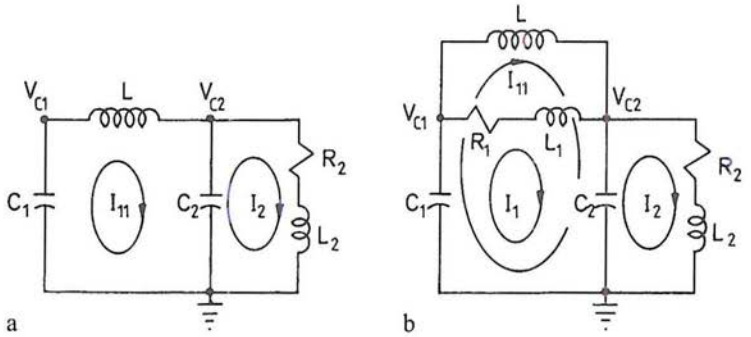

Figure 5. Equivalent circuits for the different operation steps of the Blumlein circuit: a) $0 \leq t \leq t_B$, b) $t_B \leq t \leq t_{FIN}$

The second step ($t_B \leq t \leq t_{FIN}$):

At t_{FIN} the glow discharge in the laser head arrives at the breakdown. For this step the equivalent circuit showing the operation of the system is shown in Fig. 5b. The equations governing its performance are given as follows:

$$R_1 I_1 + \beta I_1 \frac{dL_1}{dt} + L_1 \frac{dI_1}{dt} + \frac{1}{C_1} \int_{t_B}^{t_{FIN}} (I_1 + I_{11})\, dt + V_1|_{t=t_B} + \frac{1}{C_2} \int_{t_B}^{t_{FIN}} (I_1 + I_{11} - I_2)\, dt + V_2|_{t=t_B} = 0 \tag{8}$$

$$L \frac{dI_{11}}{dt} + \frac{1}{C_1} \int_{t_B}^{t_{FIN}} (I_1 + I_{11})\, dt + V_1|_{t=t_B} + \frac{1}{C_2} \int_{t_B}^{t_{FIN}} (I_1 + I_{11} - I_2)\, dt + V_2|_{t=t_B} = 0 \tag{9}$$

$$R_2 I_2 + \beta I_2 \frac{dL_2}{dt} + L_2 \frac{dI_2}{dt} + \frac{1}{C_2} \int_{t_B}^{t_{FIN}} (I_2 - I_1 - I_{11})\, dt + V_2|_{t=t_B} = 0 \tag{10}$$

where:

$$\beta = \begin{cases} 0 & \text{for } L_{der} \\ 1 & \text{for } L_{int}. \end{cases}$$

3. Parametric identification

The parametric identification is accomplished through a comparison of values

sider n experimental voltage values for $V_1^*(t_k)$ and for $V_2^*(t_k)$ $(k = 1, 2, \ldots, n)$, satisfying Eqs. (6)–(10). We have then

$$V_1 = \frac{1}{C_1}\int_0^t (\alpha I_1 + I_{11})\,dt + V_1(0) \tag{11}$$

$$V_2 = \frac{1}{C_2}\int_0^t (I_2 - \alpha I_1 - I_{11})\,dt + V_2(0) \tag{12}$$

where

$$\alpha = \begin{cases} 0 & \text{for } 0 \le t < t_B \\ 1 & \text{for } t_B \le t \le t_{FIN} \end{cases} \tag{13}$$

and where t_B can be obtained from:

$$t_B = \left\{ t \in [0, t_{FIN}] : \frac{1}{C_1}\int_0^t I_{11}\,dt + V_{C1}|_{t=0} - \frac{1}{C_2}\int_0^t (I_2 - I_{11})\,dt - V_{C2}|_{t=0} + V_B \right\} \tag{14}$$

with V_B being the measured value, I_2 and I_{11} calculated through a Runge–Kutta method, until Eq. (15) is satisfied for the experimental value of V_B.

As the parameter identification index we propose:

$$J = \sum_{k=1}^{n} \left[\left(\frac{1}{C_1}\int_0^{t_k} (\alpha I_1 + I_{11})\,dt + V_1(0) - V_1^*(t_k) \right)^2 + \left(\frac{1}{C_2}\int_0^{t_k} (I_2 - \alpha I_1 - I_{11})\,dt + V_2(0) - V_2^*(t_k) \right)^2 \right] \tag{15}$$

The problem is then reduced to determination of the $4(p+1)$ parameters $R_{1,i}, R_{2,i}, L_{1,i}, R_{2,i}$ for $i = 0, 1, 2, 3, \ldots, p$ that make the value of the Eq. (15) a minimum. In other words we have to obtain

$$\min_{R_1(I_1), R_2(I_2), L_1(I_1), L_2(I_2)} \sum_{k=1}^{n} \left[\left(\frac{1}{C_1}\int_0^{t_k} (\alpha I_1 + I_{11})\,dt + V_1(0) - V_1^*(t_k) \right)^2 + \left(\frac{1}{C_2}\int_0^{t_k} (I_2 - \alpha I_1 - I_{11})\,dt + V_2(0) - V_2^*(t_k) \right)^2 \right]. \tag{16}$$

The currents I_1, I_2 and I_{11} are obtained from the following equations:

$$\alpha \left[\frac{dI_1}{dt} + \frac{R_{1,p} I_1^p + R_{1,p-1} I_1^{p-1} + \ldots + R_{1,1} I_1 + R_{1,0}}{B_1} I_1 + \frac{1}{B_1 C_1}\int_0^{t_{FIN}} (I_1 + I_{11})\,dt + \frac{1}{B_1} V_1 \Big|_{t=0} + \frac{1}{B_2 C_2}\int_0^{t_{FIN}} (I_1 + I_{11} - I_2)\,dt + \frac{1}{B_2} V_2 \Big| \right] = 0 \tag{17}$$

$$\frac{dI_{11}}{dt} + \frac{1}{LC_1}\int_0^{t_{FIN}} (\alpha I_1 + I_{11})\,dt + \frac{1}{L}V_1\Big|_{t=0} + \frac{1}{LC_2}\int_0^{t_{FIN}} (\alpha I_1 + I_{11} - I_2)\,dt + \frac{1}{L}V_2\Big|_{t=0} = 0 \tag{18}$$

$$\frac{dI_2}{dt} + \frac{R_{2,p}I_2^p + R_{2,p-1}I_2^{p-1} + \ldots + R_{2,1}I_2 + R_{2,0}}{B_2} I_2 + \frac{1}{B_2C_2}\int_0^{t_{FIN}} (I_2 - \alpha I_1 - I_{11})\,dt + \frac{1}{B_2}V_2\Big|_{t=0} = 0 \tag{19}$$

where:

$$B_1 = (\beta p + 1)L_{1,p}I_1^p + [\beta(p-1)+1]L_{1,p-1}I_1^{p-1} + [\beta(p-2)+1]L_{1,p-2}I_1^{p-2} + \ldots + (\beta+1)L_{1,1}I_1 + L_{1,0} \tag{20}$$

$$B_2 = (\beta p + 1)L_{2,p}I_2^p + [\beta(p-1)+1]L_{2,p-1}I_2^{p-1} + [\beta(p-2)+1]L_{2,p-2}I_2^{p-2} + \ldots + (\beta+1)L_{2,1}I_2 + L_{2,0}. \tag{21}$$

4. The proposed algorithm and the results

We have used an algorithm based on the Gauss–Seidel method (see Luenberger, 1984; Bakhvalov, 1977; Niewierowicz et al., 1995), which consists of changing the value of only one parameter, holding the other $(p-1)$ as constants, until the minimal value of the optimisation index, Eq. (15), for this parameter is obtained. The changes in the parameter values are carried out using an increasing or decreasing constant. All the other parameters are treated similarly until a first cycle is completed. A second or more cycles could be done, always with smaller increasing or decreasing constant, until the increasing or decreasing constant is lower than a minimal predetermined value. This minimal predetermined constant gives the accuracy of the calculated values. Because the solution of the Eq. (15) needs the solution of the currents in the circuit, each time the parametric identification is done, the current values are obtained solving the mathematical model given by Eqs. (17)–(21), with the resistance and inductance values calculated from Eqs. (1)(2)(4)(5).

The algorithm was written in FORTRAN and a PC Pentium (200 MHz) was used. We have calculated the parametric optimisation indexes and the resistances and inductances, and for both inductance approximations (Eqs. 3) we have considered the same initial values. The solution takes the maximum time of 8 hours.

From the experimental voltage (see Fig. 3) we chose 26 values for calculation. After processing with V_k, t_k, for $k = 1, 2, \ldots, 26$, we obtained the parameter values shown in Table I, where those related to $\beta = 0$ are larger than those related to $\beta = 1$.

Fig. 6 shows the time behaviour of the resistance and inductance of each

the discharge, but after the laser emission the laser discharge changes into an arc discharge, changing the inductance and resistance drastically. Because this discharge period is not interesting for laser emission it has not been analysed.

Because a pulsed gas discharge is a dynamical process, the resistance and inductance are time dependent; physically, they are functions of the plasma conditions and their geometrical dimensions. Fig. 6 shows that the temporal behaviour of the corresponding resistances, i.e. the L and R curve inflexions take place at the same time but in the contrary sense.

In the formation phase of the discharge in the spark gap and in the laser head their resistance drops from an open circuit until a minimum, as a consequence of the electron avalanche multiplication, while their inductances rise from zero to a maximum, which depends on the geometrical evolution of the discharge. The minimal value of the inductance corresponds to the static value of the circuit components. After this formation phase, where a great part of energy in the circuit has been expanded, a glow discharge is formed and laser action takes place (approximately in the interval from 23 ns to 30 ns). So, the resistance and inductance time variations of both discharges are strongly dependent on the electrical energy in the circuit. The circuit stops working when all the energy has been consumed.

The time evolution of the inductances calculated using equations (3a) and (3b) do not show any qualitative difference, but Fig. 6 shows a better-behaved time dependence of R_{1int} than of R_{1der}.

β	i	5	4	3	2	1	0
1	$R_{1,i}$	0	2.72E−16	1.34E−11	8.05E−9	6.94E−5	1.880
	$R_{2,i}$	0	−7.30E−16	2.05E−11	−2.63E−8	−4.42E−5	1.401
	$L_{1,i}$	0	0	0	1.78E−16	−7.48E−13	1.46E−9
	$L_{2,i}$	0	0	0	1.20E−15	7.15E−13	1.66E−8
0	$R_{1,i}$	0	4.55E−16	2.04E−11	6.98E−8	9.79E−5	1.672
	$R_{2,i}$	0	−1.49E−15	2.37E−11	−3.10E−8	−5.40E−5	1.439
	$L_{1,i}$	0	0	0	9.79E−16	−9.70E−13	1.23E−9
	$L_{2,i}$	0	0	0	1.52E−15	9.42E−13	1.93E−8

Table I. Calculated parameters for the fifth order functions used to represent R_1, R_2, L_1 and L_2

	$L_{1,0}$	$L_{2,0}$	Optimisation index
estimated [nH]	1.57	16.9	—
L_{int} [nH]	1.46	16.6	$1.4360 * 10^7$
L_{dif} [nH]	1.23	19.3	$1.4842 * 10^7$

Table II. comparison of the results of identification

Finally, Fig. 7 shows the laser voltage obtained with the parameter from

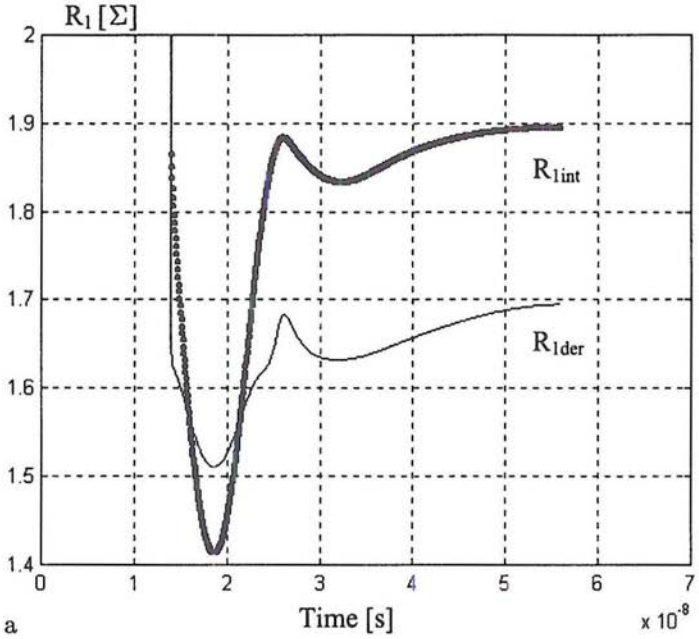

a

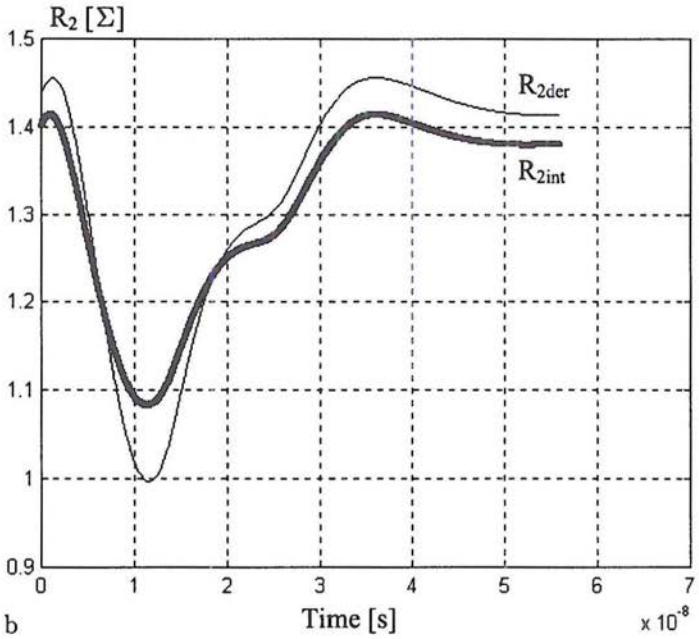

b

Figure 6. Time behaviour of the resistance and inductance of the spark gap (R_2, L_2)

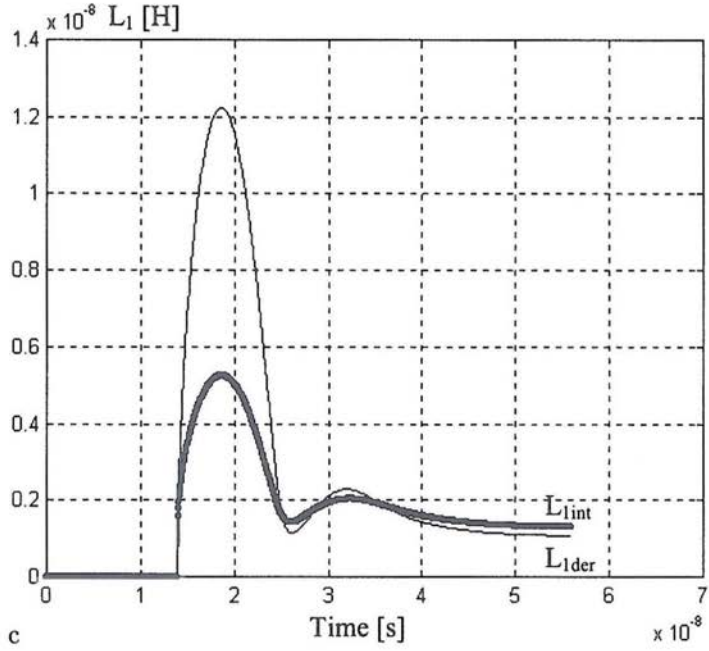
x 10^-8 L1 [H]
1.4
1.2
1
0.8
0.6
0.4
0.2
0
0 1 2 3 4 5 6 7
Time [s]
x 10^-8
L1int
L1der

c

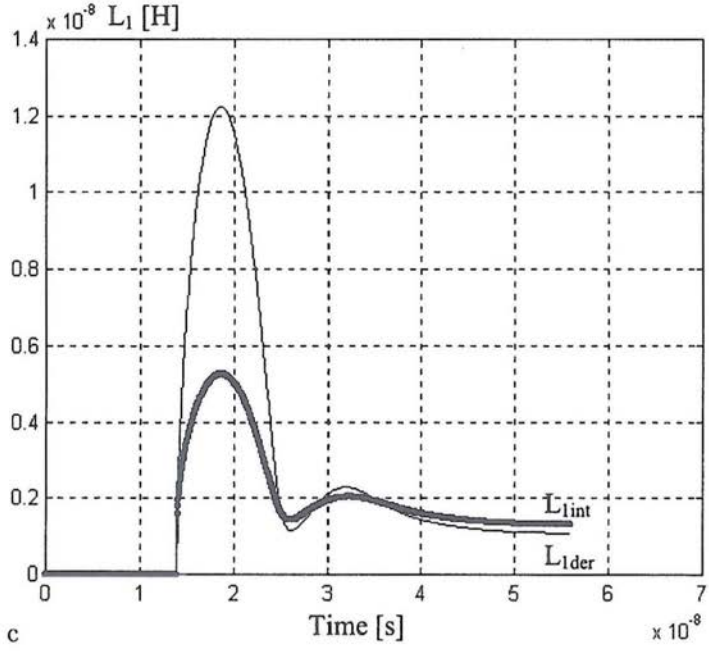
x 10^-8 L1 [H]
1.4
1.2
1
0.8
0.6
0.4
0.2
0
0 1 2 3 4 5 6 7
Time [s]
x 10^-8
L1int
L1der

c

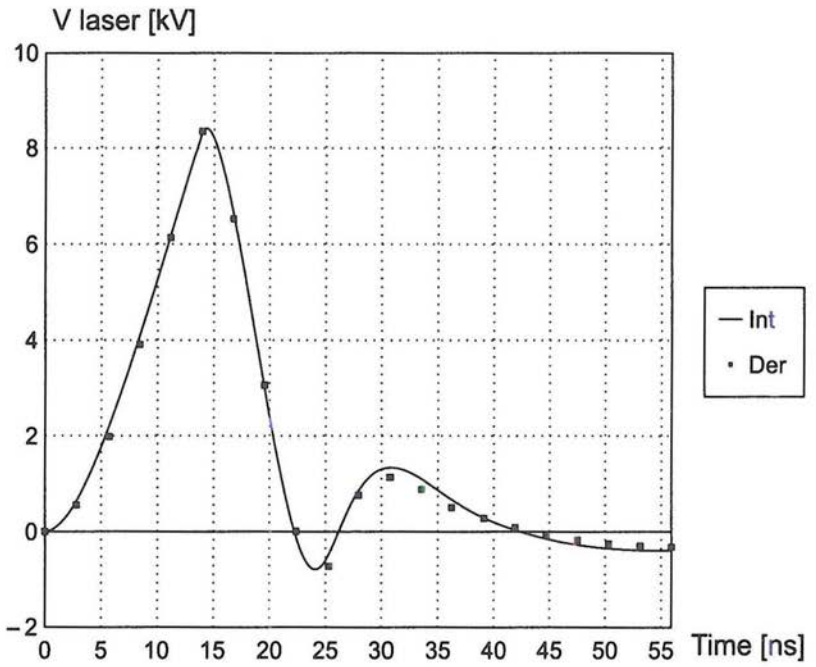

Figure 7. Simulated laser voltage

Because the parameters in Table I were calculated considering the experimental curve of Fig. 3, they satisfy the 26 values of the curve of Fig. 3, the fitting of both models is very similar.

5. Conclusions

Because the capacitor resistances R_{C1} and R_{C2} have values of the order of 0.0145 Ω (see Niewierowicz et al., 1998), the behaviour of R_1 and R_2 given in Figs. 6a,b are, respectively, the ones of the laser and the spark gap discharges. Toll (1967) found through very detailed spectroscopic measurements of the radial distribution of electron densities and gas temperatures in spark gaps a similar behaviour of the resistance in the spark channel. Then, following Toll (1967), the time behaviour of R_1 and R_2 can be explained as follows: At the very beginning both resistances are infinities because the discharges have not started, then they go down through the development of the discharges until they reach minimal values when the expansion process of the discharges stops. That is so because the energy in the circuit is not any more sufficient to sustain such expansion. Both discharges are glow discharges at that moment, and in the case

each resistance are reached, they start to grow up again till the discharges turn off when all the energy in the circuit has been exhausted.

In our previous report (see Niewierowicz et al., 1998) we have estimated, from the geometric arrangement and the material properties, the statical values for $L_{1,0} = L_{C_1} = 1.57$ nH, and $L_{2,0} = L_{C_2} + L_{SG} = 16.9$ nH. From Table II we conclude that the general Faraday law (Eq. 3a) is the best representation for the induced *emf* in the circuit loops. Physically, equation (3a) is also the best representation of the self-induced electromotive force, because the laser and the spark gap discharges in the circuit develop freely. That is, not only the current but their dimensions, as well (and after that their inductance) are time dependent.

References

BAKHVALOV, N.S. (1977) *Numerical Methods.* Mir.

GLASSTONE, S. and LOUBERG, R.H. (1960) *Controlled Thermonuclear Reactions.* Robert E. Krieger Publishing Co., Inc., 165–167.

KAWECKI, L., NIEWIEROWICZ, T. and DE LA ROSA, J. (1997) Parametric Identification of the Variable Structure Model of a N_2 Laser. *Rev. Mex. Fís.*, **43**, 2, 248–256.

LUENBERGER, D.G (1984) *Linear and Nonlinear Programming.* Addison-Wesley Publishing Company, Inc.

NIEWIEROWICZ, T., KAWECKI, L. and DE LA ROSA, J. (1995) Identification of the Electrical Parameters of a Blumlein Circuit Used in the Excitation of N_2 Lasers. *Rev. Mex. Fís.*, **41**, 6, 822–831.

NIEWIEROWICZ, T., KAWECKI, L. and DE LA ROSA, J. (1998) Parametric Identification of the Non-linear Model of a Blumlein N_2 Laser. *Rev. Mex. Fís.*, **44**, 6, 564–569.

PERSEPHONIS, P., GIANNETOS, B., PARTHENIOS, J., GEORGIADES, C. and IOANNON, A. (1995) The Time Dependent Resistance and Inductance of the Electric Discharges in Pulsed Gas Lasers. *IEEE J. Quantum Electron.*, **31**, 1779–1784.

REITZ, J.R and MILFORD, F.J. (1960) *Foundations of Electromagnetic Theory.* Addison-Wesley Publishing Company, Inc., 170–174.

DE LA ROSA, J., FONSECA, W.H., CALVA, P.A., LINARES, R. and VÁZQUEZ MARTÍNEZ, A. (1994), Longitudinal Coil for Measuring Fast Pulsed Currents Flowing Along Sheets. *Meas. Sci. Technol.*, **5**, 1109–1114.

TOLL, H. (1967) Spektroskopische Messung des zeitlichen Verlaufs der radialen Dichte- und Temperaturverteilung in einem Wasserstoffunken. *Z. Naturforsch.*, **22a**, 1068–1088.

WOJNAR, A., ed. (1969) *Poradnik Inżyniera Radioelektryka* (*A Guidebook of a Radio Engineer*; in Polish), Wydawnictwa Naukowo-Techniczne, Warszawa, 40–41.